Electronic Supplementary Information

Two-photon ratiometric fluorescent probe for real-time imaging and quantification of NO in neural stem cells during activation regulation

Mengyu Liang, Zhichao Liu*, Zhonghui Zhang, Yuxiao Mei, Yang Tian*

Department of Chemistry, School of Chemistry and Molecular Engineering, East China Normal University, Dongchuan Road 500, Shanghai 200241, China.

E-mail: ytian@chem.ecnu.edu.cn (Yang Tian), zcliu@chem.ecnu.edu.cn (Zhichao Liu)

Contents

1. Reagents and Instruments

Reagents: 2,2-Dimethyl-1,3-dioxane-4,6-dione, 4-bromo-1,8-naphthalic anhydride, 2-methoxyethanol, ethylenediamine and 2,4-dihydroxybenzaldehyde were purchased from Sinopharm- Reagent (China). 2-nitro-1,4-phenylenediamine, triethylamine (TEA), palladium on carbon (Pd/C, 10% Pd), NaH_2PO_2, NaClO, $Na_2S_2O_4$, Na_2SO_4, $NaNO_2$, $NaHCO_3$, $MnCl_2·4H_2O$, NaCl, KCl, $CuCl_2·2H_2O$, $MgCl_2·6H_2O$, $CaCl_2$, $FeCl_3$ and N,N-dimethylformamide (DMF) were obtained from Aladdin Chemistry (China). 3-(4,5-dimethyl-2-thiazolyl)-2,5-diphenyl-2H-tetrazolium bromide (MTT), ascorbic acid (AA), glucose, amino acid, and dimethyl sulfoxide (DMSO) were obtained from Sigma-Aldrich (U.S.A.). 2-(4-carboxyphenyl)-4,4,5,5-tetramethyl-imidazoline-1-oxyl-3-oxide potassium (cPTIO), Threonine (Glu), Phenylalanine (Phe), Tyrosine (Tyr), Lysine (Lys), Cysteine (Cys), Histidine (His), Arginine (Arg), Valine (Val), Proline (Pro), Threonine (Thr), Serine (Ser), Leucine (Leu), Methionine (Met), Glycine (Gly). Poly-d-lysine (PDL), minimum essential medium (MEM) and phosphate-buffered saline (PBS) were obtained from Thermo Fisher Scientific. O-Benzotriazole-N, N, N', N'-tetramethyl-uronium-hexafluorophosphate (HBTU) were provided by Macklin (China).

Instruments: Milli-Q water purification system was used to purify deionized water. All NMR spectra were conducted from NMR spectrometer (500 MHz, Bruker, Germany). The Mass spectra (MS) were obtained with MS spectrometer (6800, Bruker, Germany). UV–vis absorption spectra were recorded on UV–vis spectrophotometer (UH5300, Hitachi, Japan). The fluorescence spectra were collected with fluorescence spectrophotometer (F-4500, Hitachi, Japan). Fourier transform infrared (FT-IR) spectra were performed with Fourier transform infrared spectrometer (Nicolet iS10, Thermo Fisher Scientific, U.S.A.). Fluorescence confocal imaging was collected by confocal scanning microscope with 63× oil objective (TCS-SP8, Leica, Germany).

2. Measurements of two-photon cross section and FRET efficiency.

The two-photon action cross section (σΦ) was measured by using standard materials combined with femtosecond fluorescence measurement technology and Rhodamine 6G was used as reference. Firstly, the two-photon fluorescence intensity of 10 μM NOP (10 mM PBS buffer containing ethanol, pH = 7.4) added with 50 μM NO was carried out at 690-900 nm. The two-photon action cross section (δ) was calculated by using the following equation:

$$\delta_s = \delta_r \frac{\Phi_r}{\Phi_s} \frac{C_r n_r F_s}{C_s n_s F_r}$$

Where the s and r refer to RBD and the reference solutions, respectively. The two-photon fluorescence intensity was described as F. The n and C are the refractive index and concentration of the sample solution, respectively. The Φ and δ represent the fluorescence quantum yield and the TPA cross section.

The FRET efficiency of NOP in the absence and in the presence of NO was calculated according to the following equation:

$$E = 1 - \frac{F_{DA}}{F_D}$$

E represents the FRET efficiency, F_D and F_{DA} represent the measured fluorescence intensities of the donor in the absence and in the presence of acceptor, respectively.

3. Theoretical calculation and statistical analysis.

The HOMO and LUMO of the molecules are calculated using Gaussian 09 suite. The geometry optimizations of the molecule were performed using density functional theory (DFT) with Becke's three-parameter hybrid exchange function with PBE1PBE and 6-311G basis set. No constraints to bonds/angles/dihedral angles were applied in the calculations and all atoms were free to optimize.

Data are expressed as means ± SD of 3-4 samples in each experimental group. The Student t test was used to assess the statistical significance between a pair of experimental groups. P-values were generated by two-tailed t test assuming equal variance using IBM SPSS Statistics Software. The value 0.05 (*), 0.01 (**), and 0.001 (***) was assumed as the level of significance for the statistic tests (n = 20; *, $P < 0.05$; **, $P < 0.01$; ***, $P < 0.001$; and NS means no statistical significance per unpaired t-test).

4. Characterization of NOP and intermediates (Fig. S1-S15).

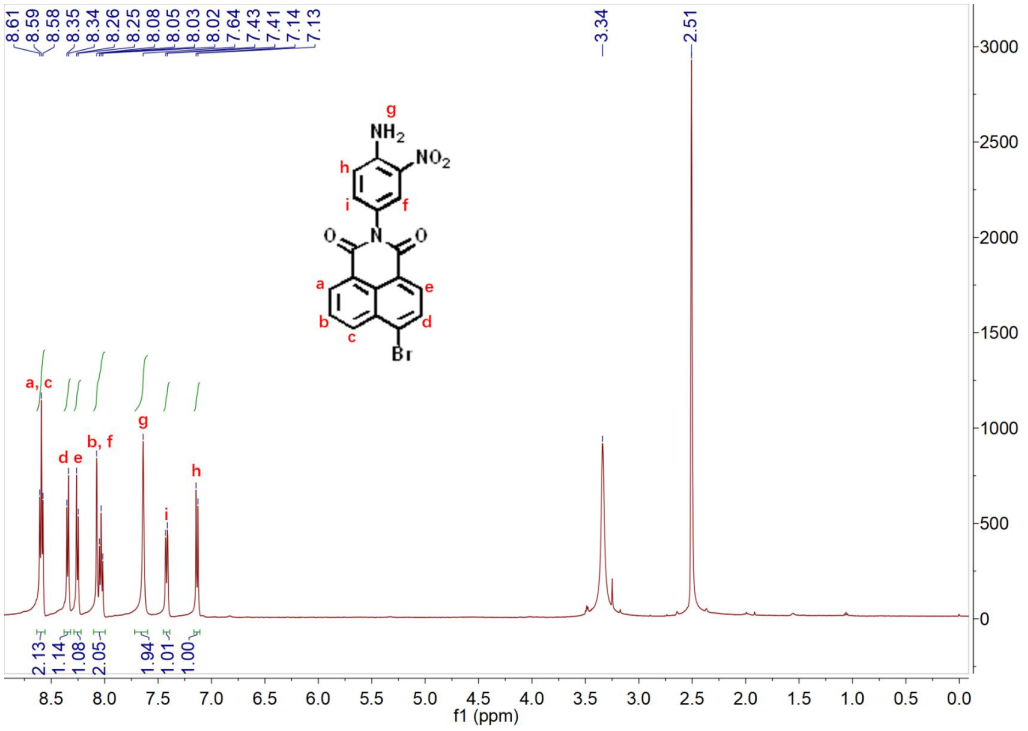

Fig. S1 ^{1}H NMR spectrum (500 MHz) of compound 1 in DMSO-d_6.

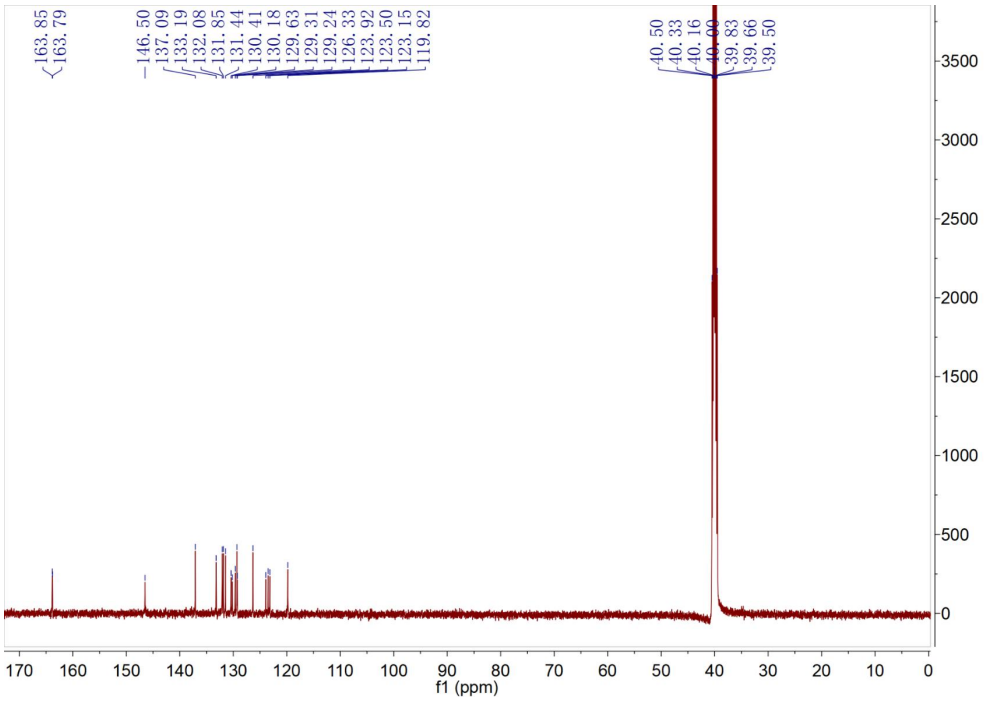

Fig. S2 ^{13}C NMR spectrum (500 MHz) of compound 1 in DMSO-d_6.

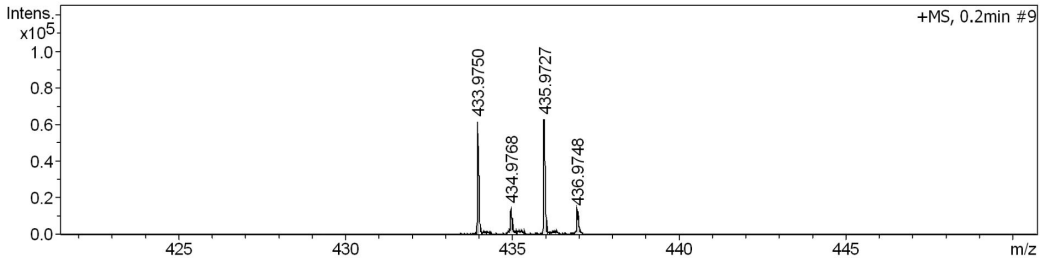

Fig. S3 MS spectrum of compound 1.

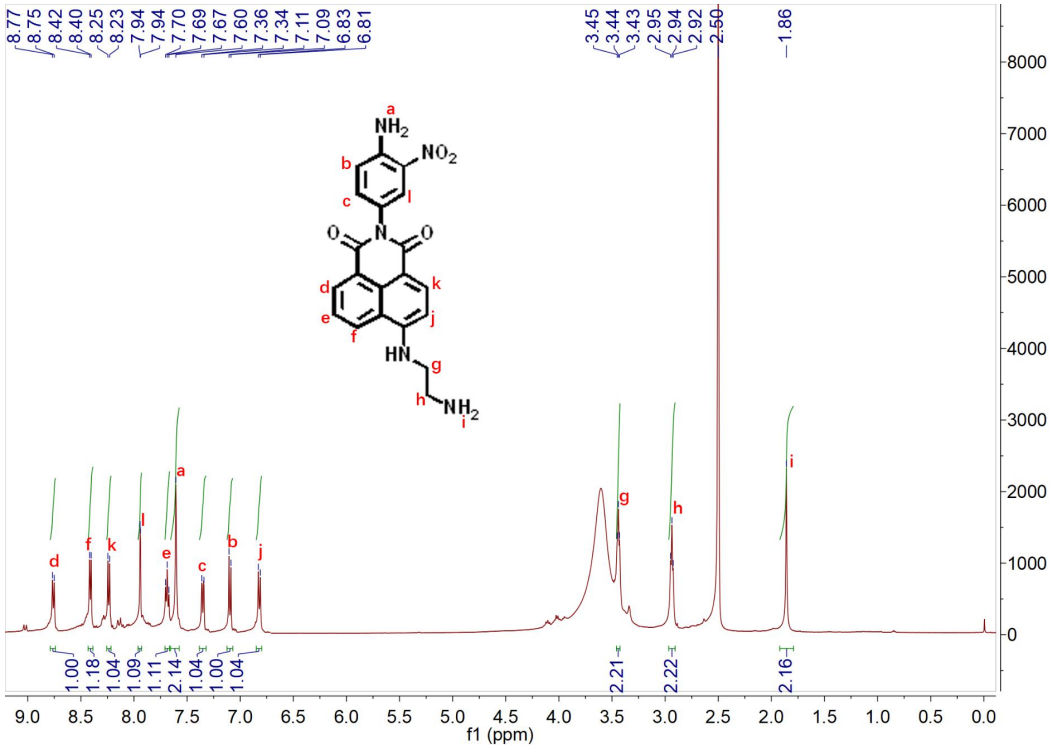

Fig. S4 ^{1}H NMR spectrum (500 MHz) of compound 2 in DMSO-d_6.

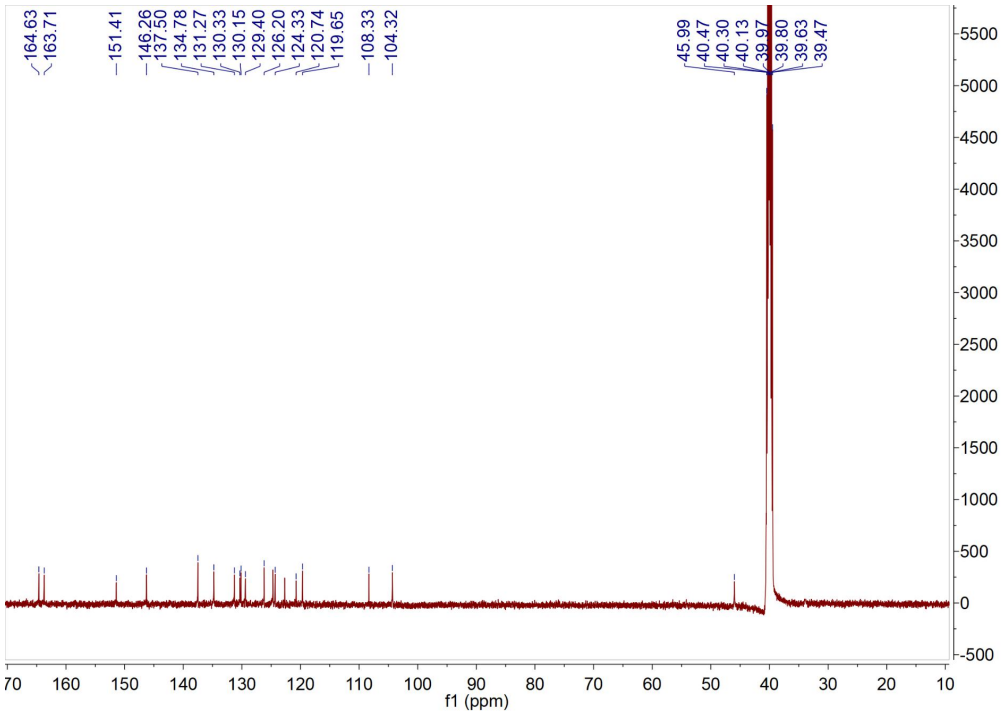

Fig. S5 ^{13}C NMR spectrum (500 MHz) of compound 2 in DMSO-d_6.

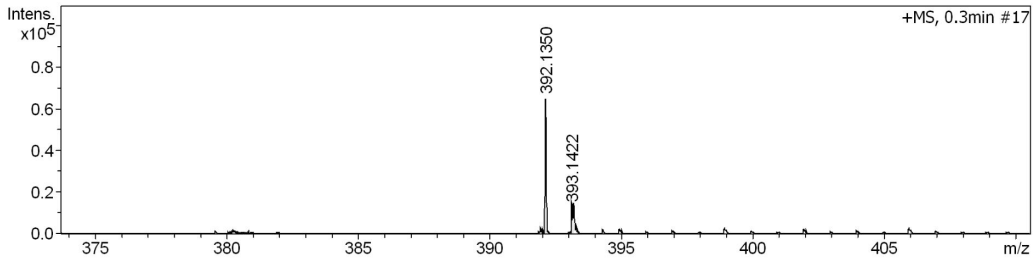

Fig. S6 MS spectrum of compound 2.

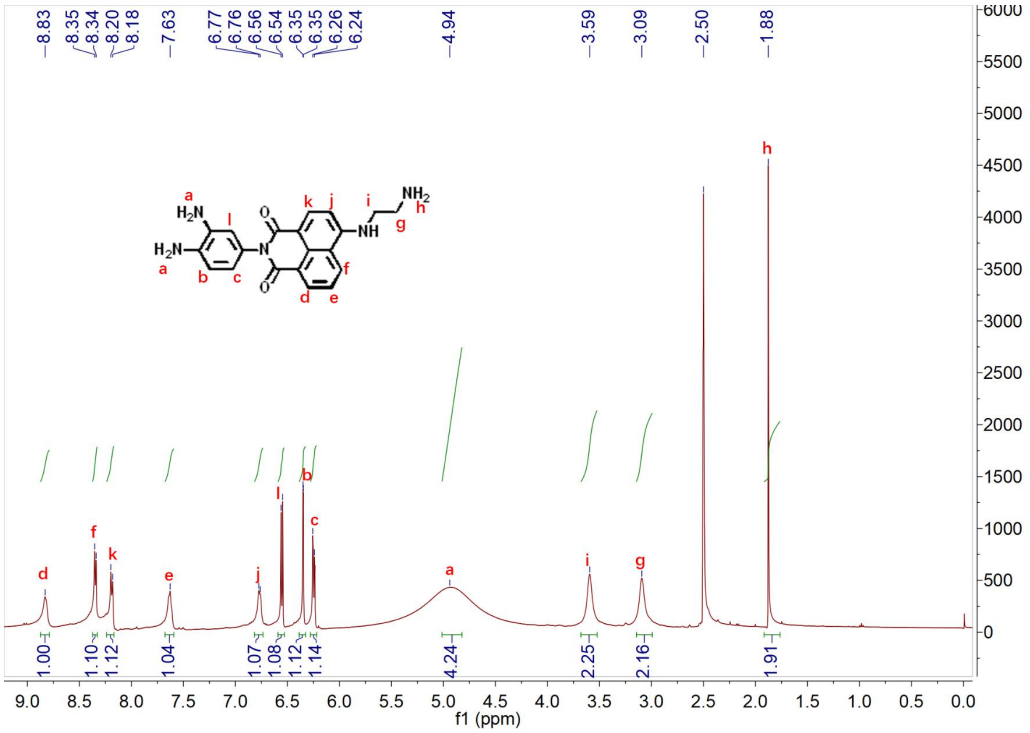

Fig. S7 ^{1}H NMR spectrum (500 MHz) of NPM in DMSO-d_6.

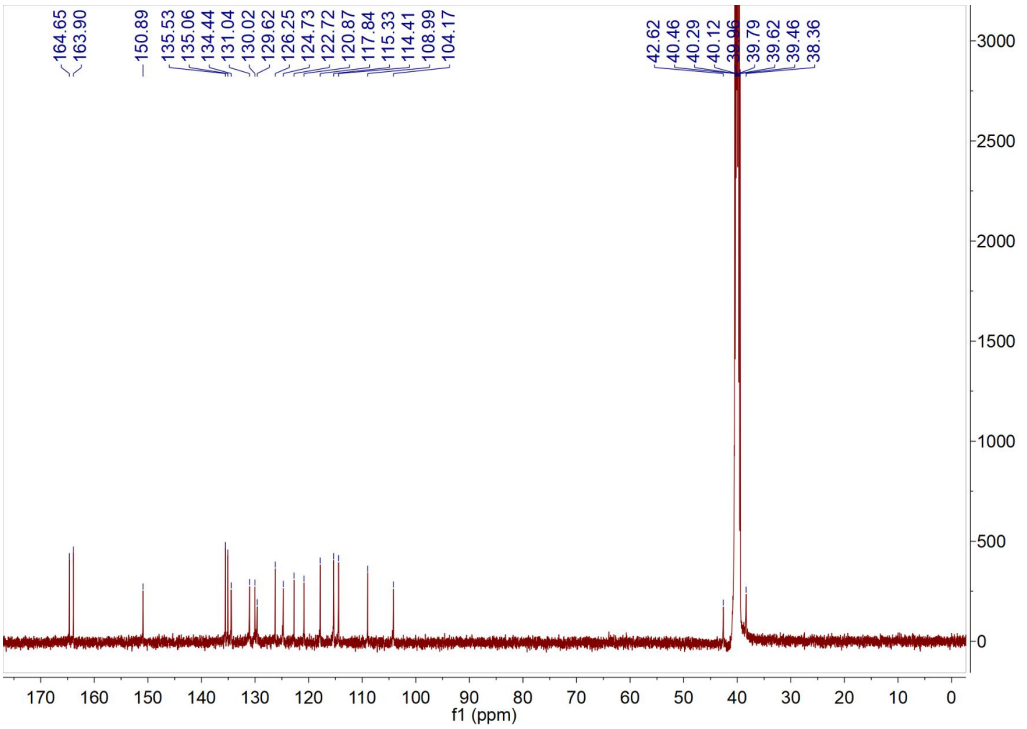

Fig. S8 ^{13}C NMR spectrum (500 MHz) of NPM in DMSO-d_6.

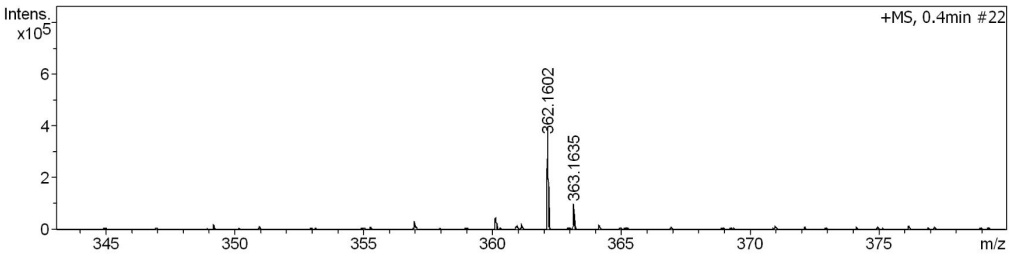

Fig. S9 MS spectrum of NPM.

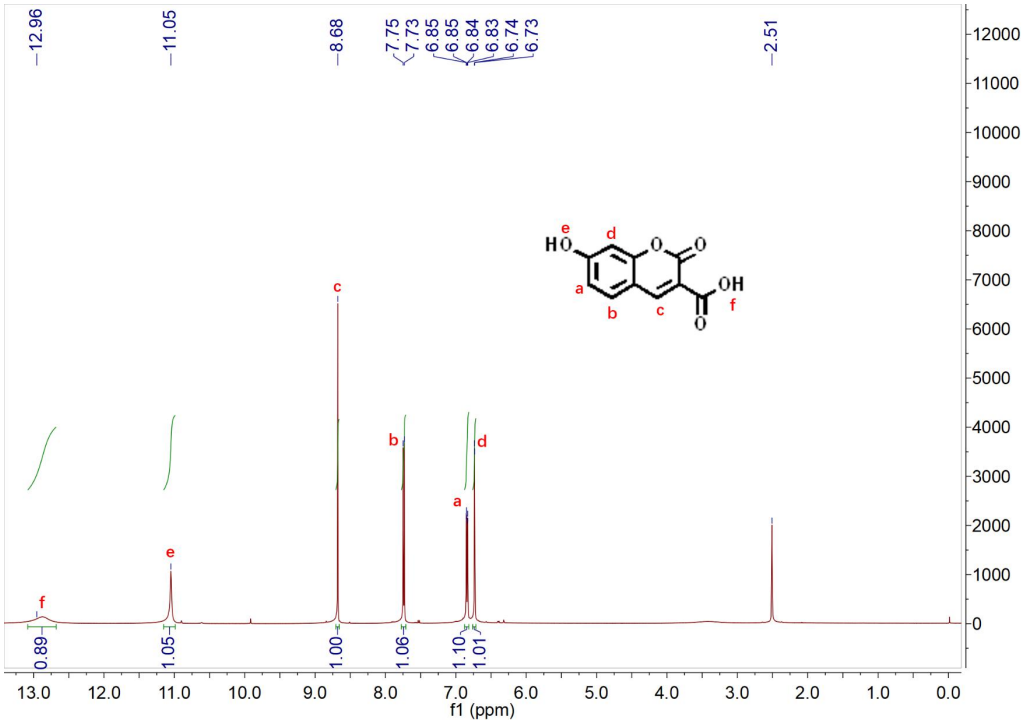

Fig. S10 ^{1}H NMR spectrum (500 MHz) of CM in DMSO-d_6.

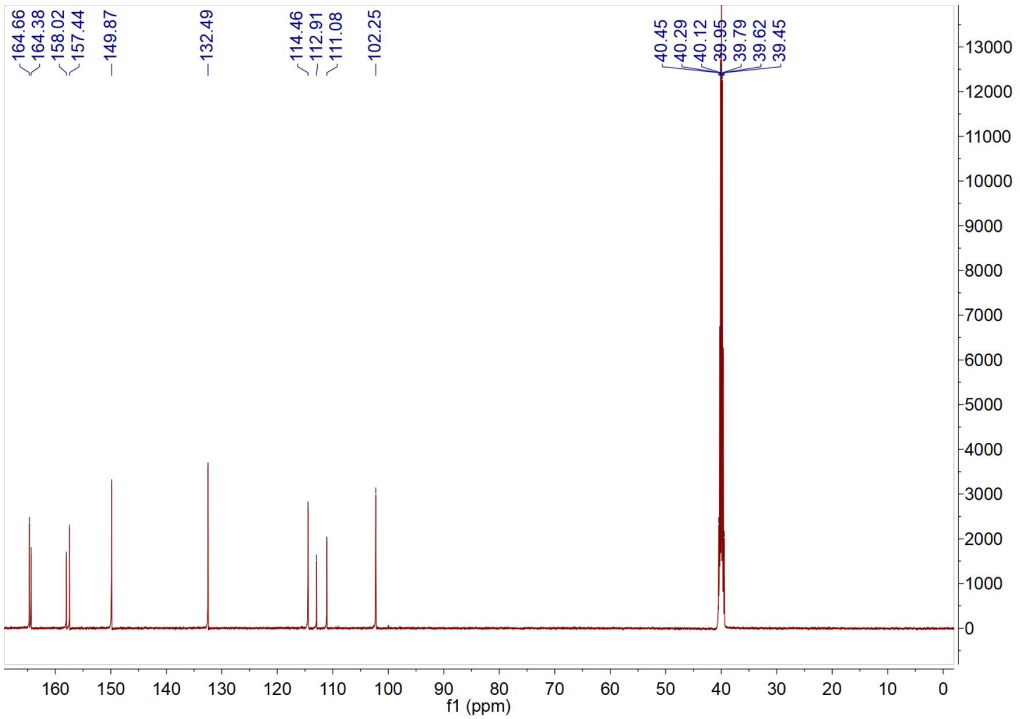

Fig. S11 ^{13}C NMR spectrum (500 MHz) of CM in DMSO-d_6.

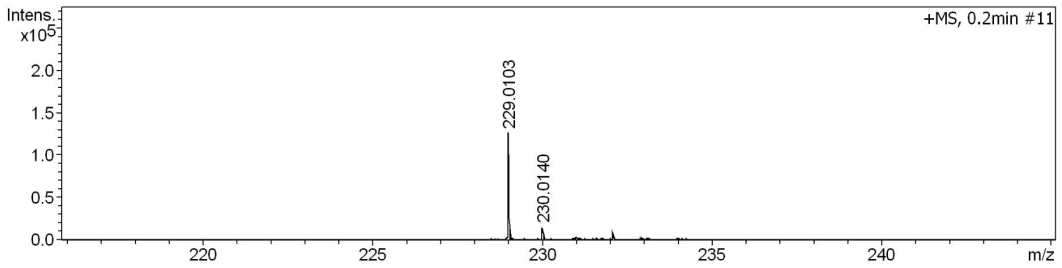

Fig. S12 MS spectrum of CM.

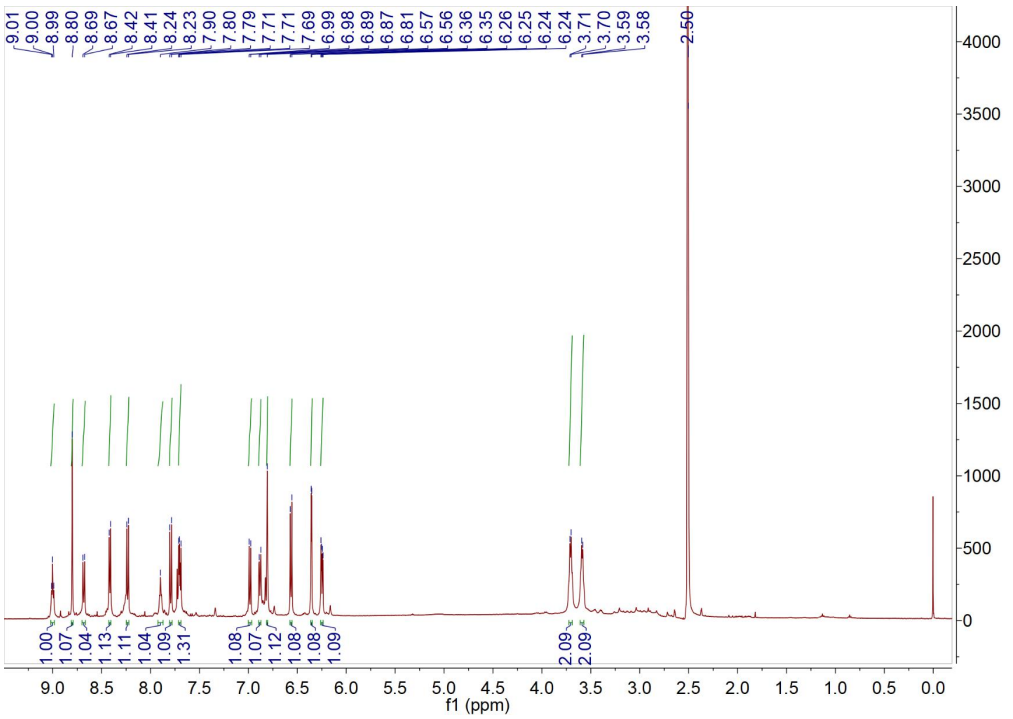

Fig. S13 ^{1}H NMR spectrum (500 MHz) of NOP in DMSO-d_6.

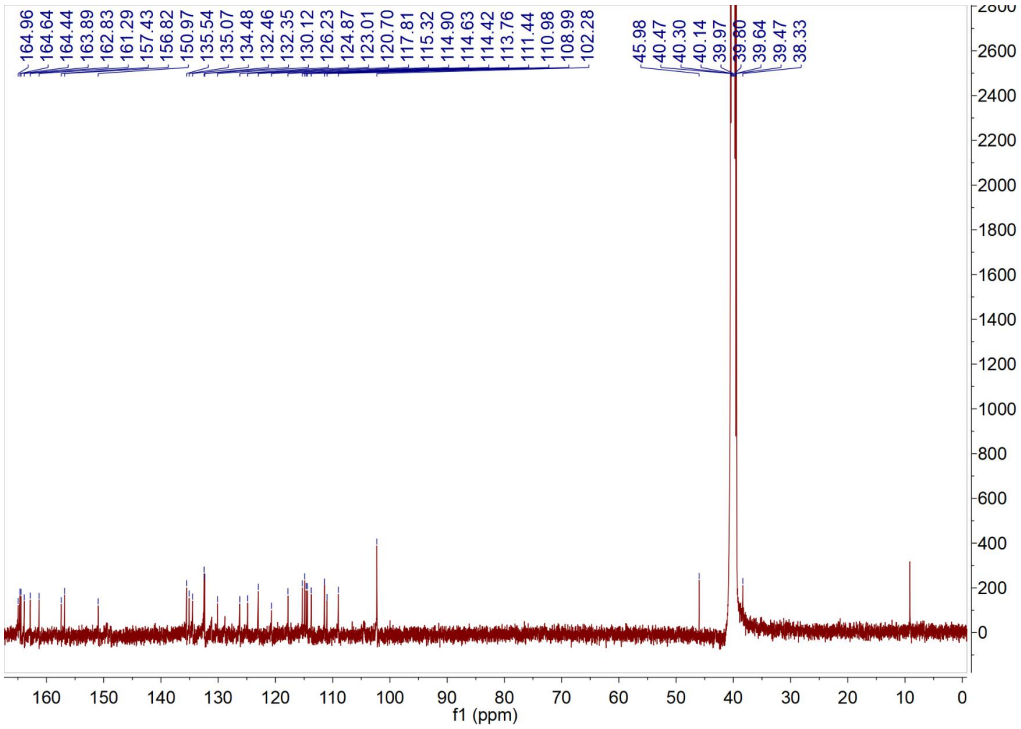

Fig. S14 ^{13}C NMR spectrum (500 MHz) of NOP in DMSO-d_6.

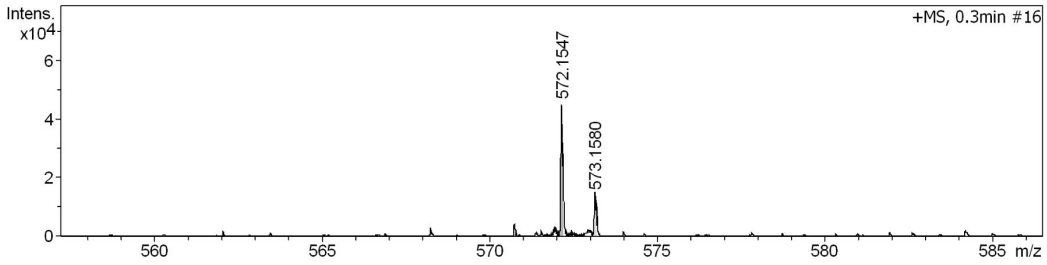

Fig. S15 MS spectrum of NOP.

5. The two-photon fluorescence emission spectra of NOP in cell lysates and cell lysates only (Fig. S16).

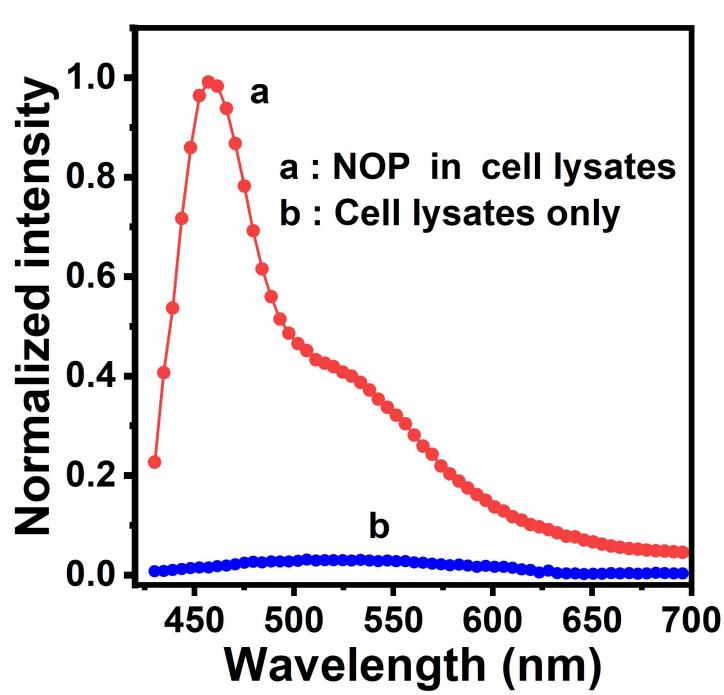

Fig. S16 TPF emission spectra of (a) NOP in cell lysates and (b) cell lysates only under the excitation of 700 nm, respectively.

6. Selectivity and competition tests of NOP toward metal ions, amino acids and neurotransmitters (Fig. S17).

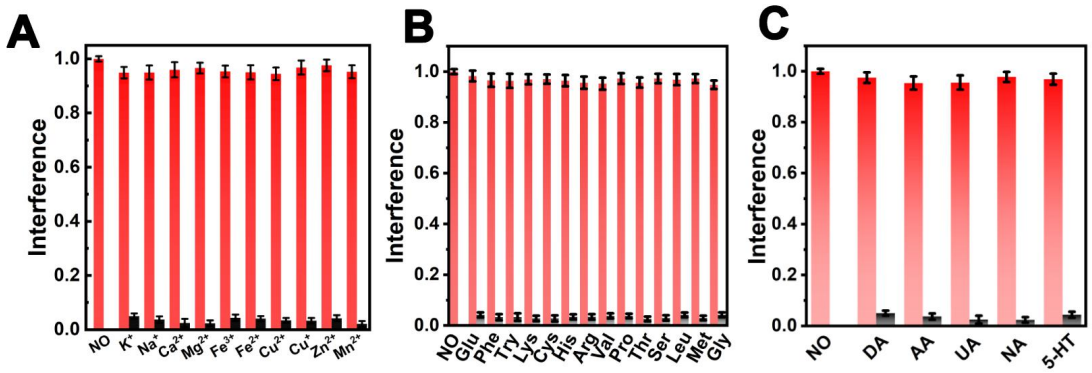

Fig. S17 Selectivity and competition tests of NOP toward (A) metal ions, (B) amino acids (100 μM) and (C) neurotransmitters (50 μM), respectively. The black bars represent the influence of potential interferences to NOP probe. The red bars represent the subsequent addition of 100 μM NO to the NOP solution with potential interferences. The concentrations of K^+, Na^+ and Ca^{2+}: 100 mM, 50 mM and 10 mM, respectively. The concentration of Mg^{2+}, Fe^{3+}, Fe^{2+}, Cu^{2+}, Cu^+, Zn^{2+}, Mn^{2+}: 300 μM.

7. Two-photon fluorescence emission spectra of CM and NOP (Fig. S19).

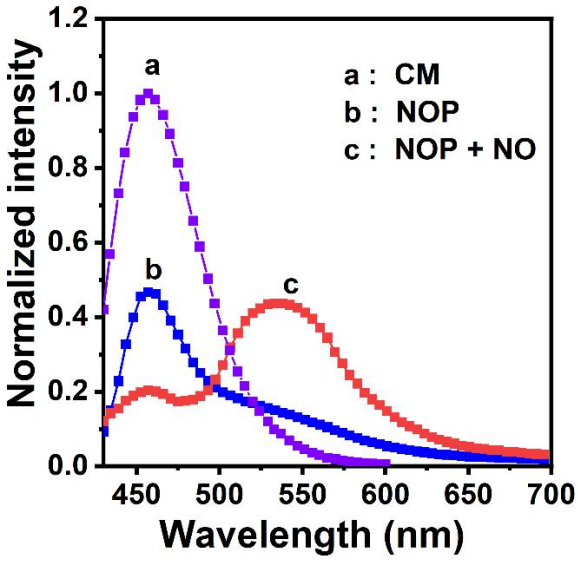

Fig. S18 Two-photon fluorescence emission spectra of (a) CM, (b) NOP in the absence and (c) in the presence of NO (200.0 μM), respectively.

8. The structures of NOP before and after reacted with NO (Fig. S18).

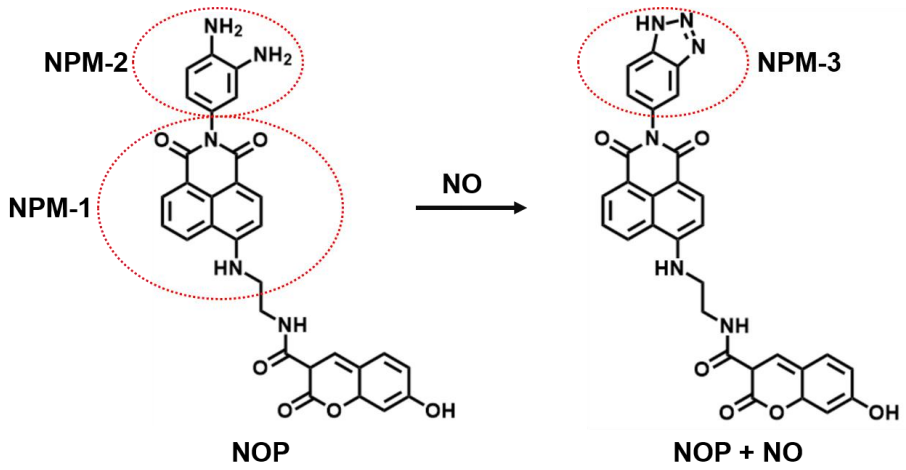

Fig. S19 Molecule structures of NOP before and after reacted with NO, respectively.

9. Cytotoxicity and apoptosis assay of NOP probe (Fig. S20-S22).

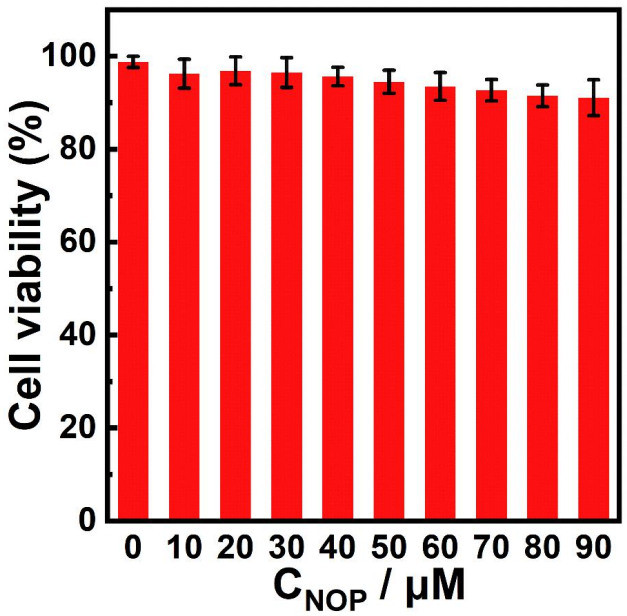

Fig. S20 Viabilities of NSCs after incubated with different concentrations of NOP probe for 48 h at 37 ºC, respectively.

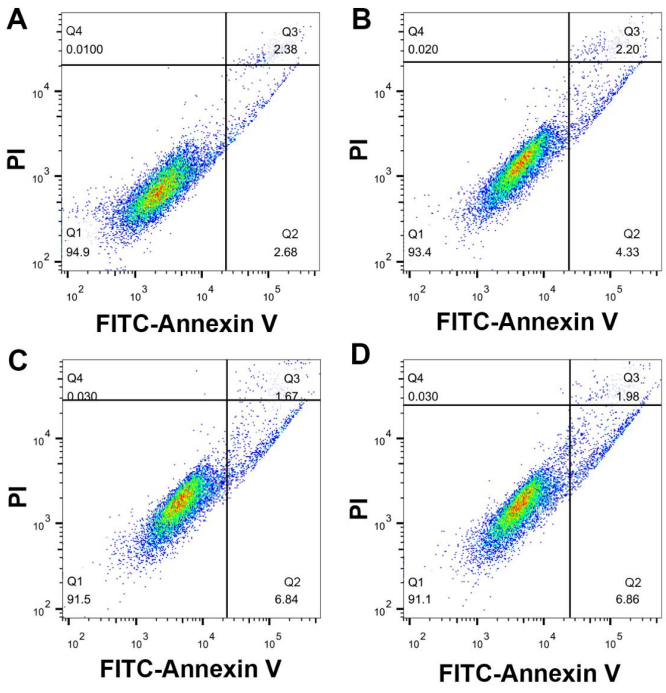

Fig. S21 Cell apoptosis assay of NSCs after incubated with different concentrations of NOP for 48 h (A) 0 μM, (B) 30 μM, (C) 60 μM, (D) 90 μM. Q1, Q2, Q3 and Q4 represent living cells, early apoptotic cells, late apoptotic cells, and dead cells, respectively.

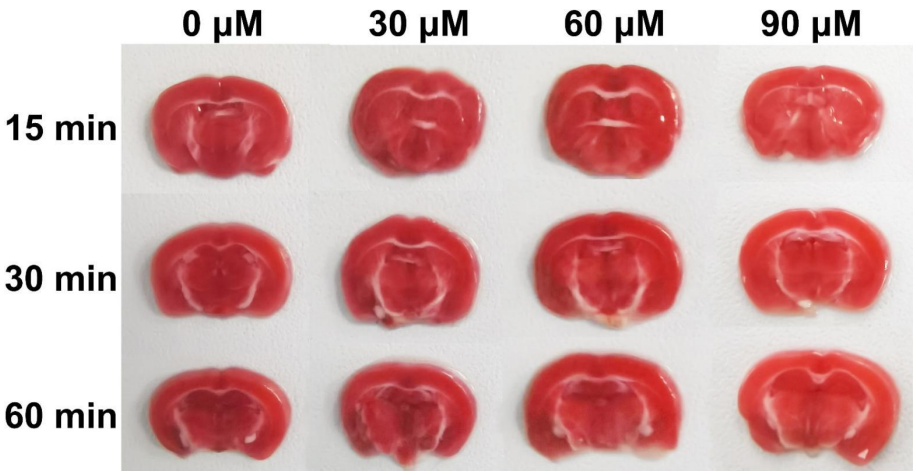

Fig. S22 TTC staining of brain tissues obtained from the live mouse brain after incubated with different concentrations of NOP (0, 30, 60, 90 μM) for different times (15, 30 and 60 min)

10. Western blot of EGFR and CD133 proteins in the used qNSCs (Fig. S23).

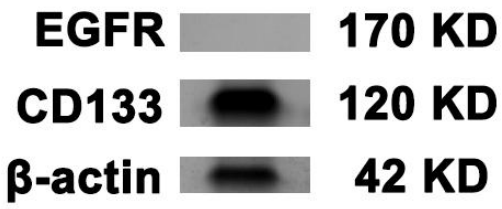

Fig. S23 Western blot analysis for the levels of EGFR and CD133 proteins in the used qNSCs.

11. Fluorescence imaging of NSCs (Fig. S24-S25).

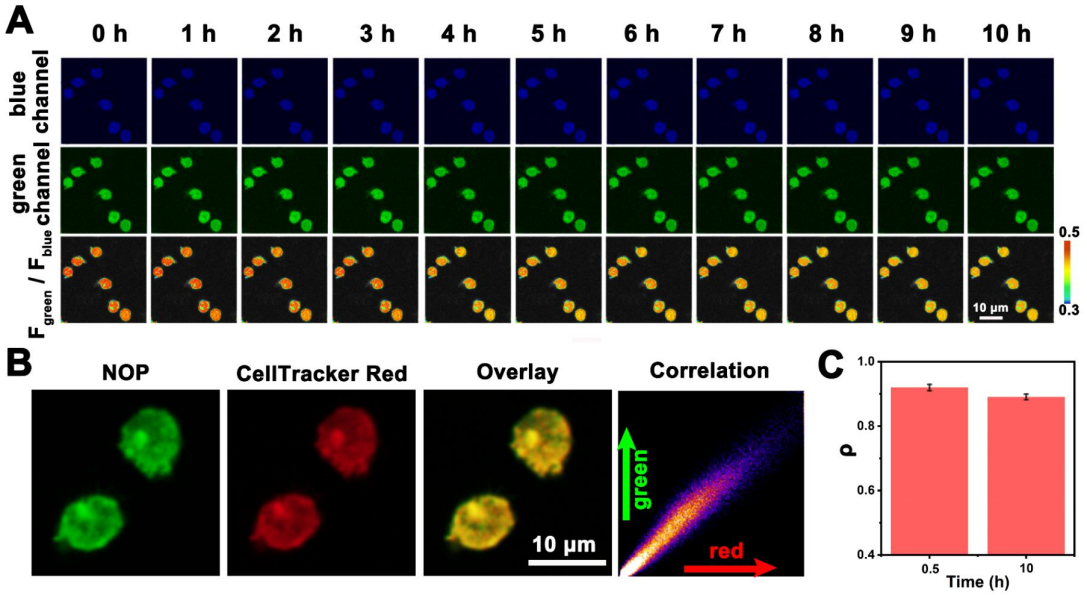

Fig. S24 (A) Fluorescence imaging of NSCs treated with NOP (10 μM) for 20 min and collected from blue, green and F_{green}/F_{blue} channels. (B) Colocalization images of qNSCs incubated with NOP and CellTracker Red for 10 h. (C) Pearson's coefficient (ρ) obtained from incubated with NOP and CellTracker Red for 0.5 h and 10 h.

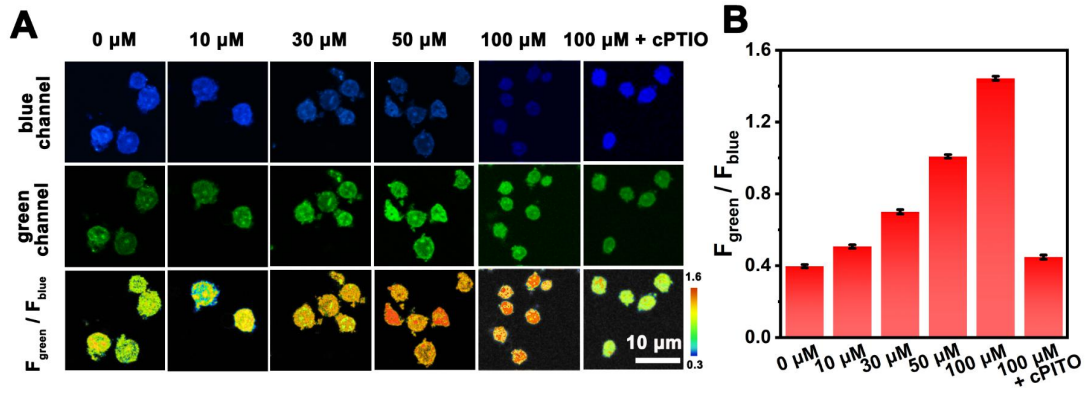

Fig. S25 (A) Fluorescence imaging of NSCs incubated with NOP probe collected from different channels under the stimulation of different concentrations of NO (0, 10, 30, 50, and 100 μM), and 100 μM NO in the presence of cPTIO (150 μM). (B) Summarized data for F_{green}/F_{blue} value obtained from (A).

12. Neurotoxicity of NO toward NSCs (Fig. S26).

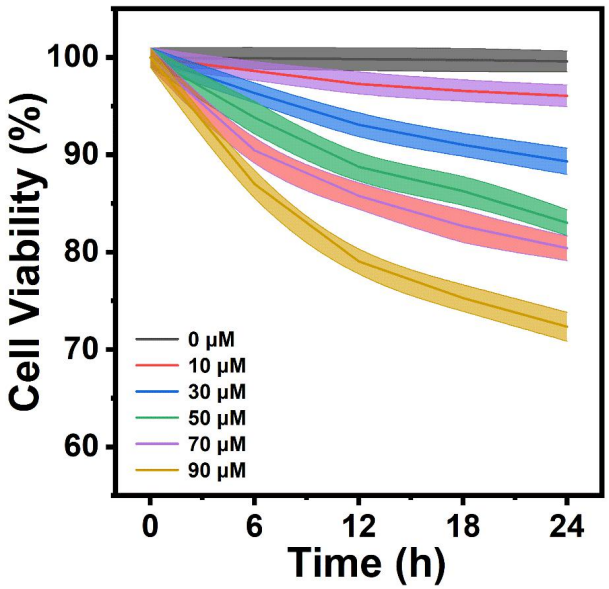

Fig. S26 Summarized data of NSCs viability stimulated by different concentrations of NO (0, 10, 30, 50, 70, 90 μM) for different times (0, 6, 12, 18, 24 h).

13. FACS of qNSCs (Fig. S27).

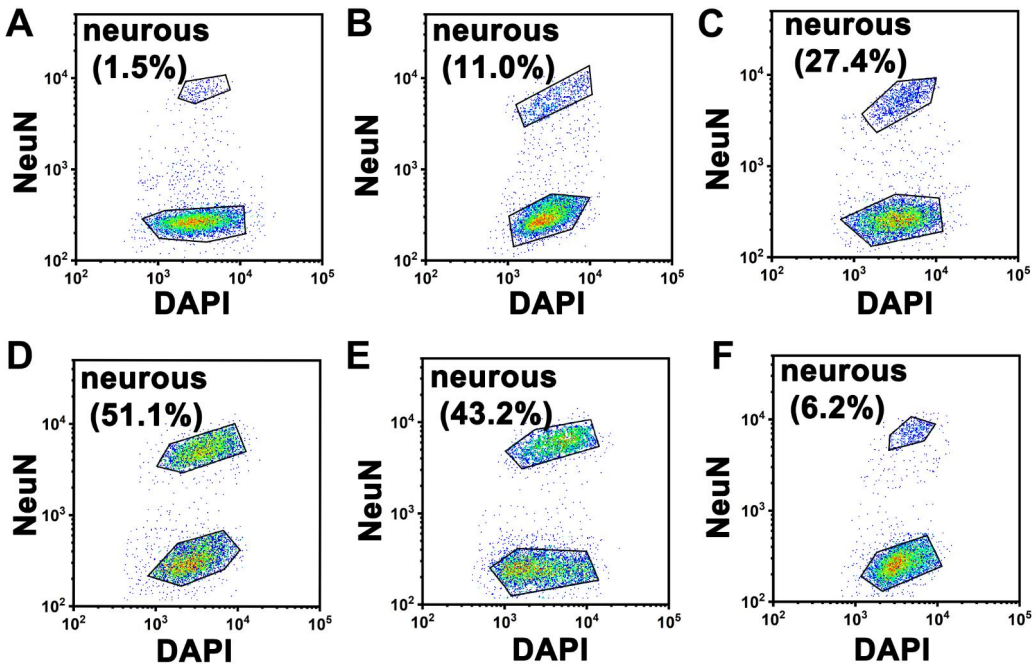

Fig. S27 FACS results of qNSCs after stimulated by (A) 0 μM, (B) 10 μM, (C) 30 μM, (D) 50 μM, (E) 70 μM of NO, and (F) 70 μM of NO in the presence of cPTIO for 300 s, and then the stimulated qNSCs were cultured for 24 h (n=5, S. D.).

14. Histology aligned to Allen Brain Atlas (Fig. S28).

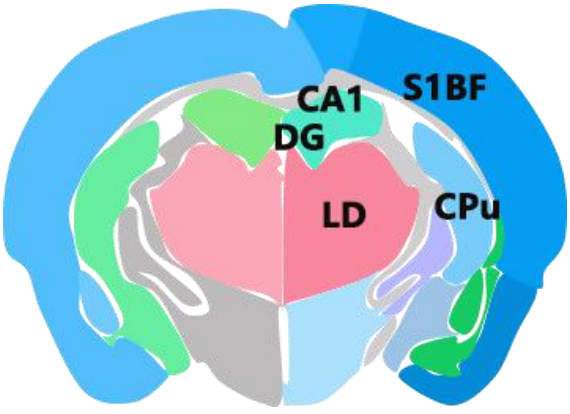

Fig. S28 Histology aligned to Allen Brain Atlas.

15. The concentration of NO in qNSCs and neurons (Fig. S29).

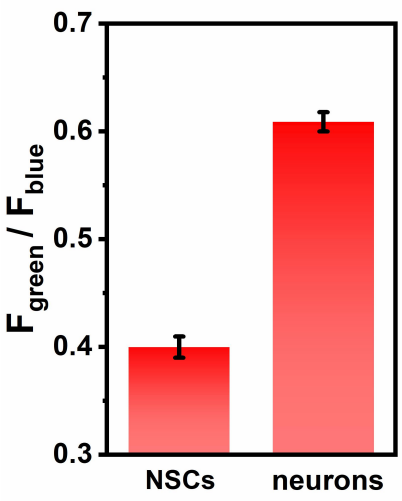

Fig. S29 Summarized data for F_{green}/F_{blue} value obtained from qNSCs and neurons. (n=50, S. D.)

16. FACS of cells obtained from DG area (Fig. S30)

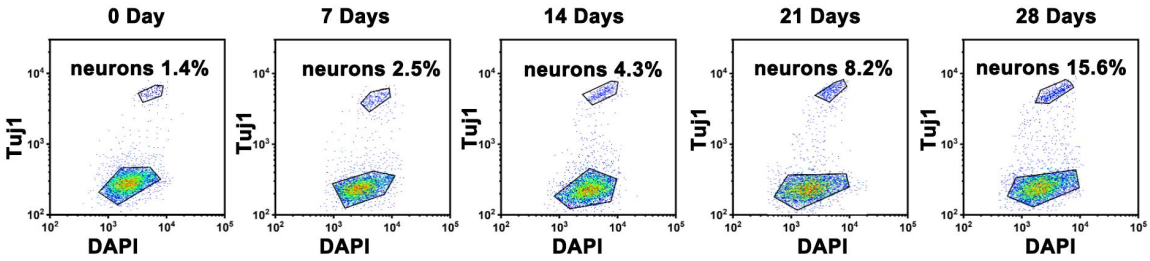

Fig. S30 FACS results of cells obtained from DG area after the AD mice were treated with aNSCs for different times (0, 7, 14, 21 and 28 days), respectively.

17. The comparison of the sensing properties of our developed NOP probe and the previously reported fluorescent ratiometric NO probes.

Table S1. The comparison of the sensing properties of our developed NOP probe and the previously reported fluorescent ratiometric NO probes.

Probes	Response time	Detection Liner range	Detection limit	References
TRP-NO	50 min	5.0-160.0 μM	1.8 μM	S1
Prober 1	10 min	0.0-20.0 μM	17.0 nM	S2
Cu (FL3A-Ppz-CC)	2 min	0.0-6.0 μM	21.0 nM	S3
AC-SA	15 min	0.0-700.0 nM	4.05 nM	S4
Rh-NO-P	20 s	0.5-12.0 μM	51.3 nM	S5
Hoe-Rh-NO	20 s	0.0-40.0 μM	58.0 nM	S6
FP-NO	20 s	0.25-2.00 μM	47.6 nM	S7
Mito-N	20 min	0.0-40.0 μM	21.0 μM	S8
RBD@AuNCs	55 s	0.5-120.0 μM	105.0 nM	S9
NOP	15 s	0.100-200 μM	19.5 nM	Our work

References:

[S1] Z. Dai, L. Tian, B. Song, X. Liu and J. Yuan, *Chem. Sci*., 2017, 8, 1969-1976.

[S2] L. Chen, D. Wu and J. Yoon, *Sens. Actuators B Chem*., 2018, 259, 347-353.

[S3] A. Loas and S. J. Lippard, *J. Mater. Chem. B*, 2017, 5, 8929-8933.

[S4] P. Liu, B. Li, J. Zheng, Q. Liang, C. Wu, L. Huang, P. Zhang, Y. Jia, and S. Wang, *Sens. Actuators B Chem*., 2021, 329, 129147.

[S5] X. Wang, Q. Sun, X. Song, Y. Wang and W. Hu, *RSC Adv.*, 2022, 12, 2721-2728.

[S6] L. Zhao, Z. Huang, D. Ma, Y. Yan, X. Zhang and Y. Xiao, *Analyst*, 2021, 146, 4130-4134.

[S7] Q. Han, J. Liu, Q. Meng, Y. Wang, H. Feng, Z. Zhang, Z. Xu and R. Zhang, *ACS Sens*., 2019, 4, 309-316.

[S8] X. Zhu, J. Chen, C. Ma, X. Liu, X. Cao and H. Zhang, *Analyst*, 2017, 142, 4623-4628.

[S9] Z. Gong, Z. Liu, Z. Zhang, Y. Mei and Y. Tian, *CCS chem.*, 2021, 3, 2201-2211.